Liquid Crystals
Publication details, including instructions for authors and subscription information:
http://www.informaworld.com/smpp/title~content=t713926090

New mesomorphic organocyclosiloxanes II. Thermal behaviour and mesophase structure of organocyclohexasiloxanes

Elena V. Matukhina Corresponding author[a]; Olga I. Shchegolikhina[b]; Yulia A. Molodtsova[b]; Yulia A. Pozdniakova[b]; Konstantin A. Lyssenko[b]; Viktor G. Vasil'ev[b]; Mikhail I. Buzin[b]; Dimitris E. Katsoulis[c]
[a] Department of Physics, Moscow State Pedagogical University, Moscow 119882, Russia [b] Institute of Organoelement Compounds, Russian Academy of Sciences, Moscow 119991, Russia [c] Dow Corning Corporation, Midland MI 48686, USA

Online publication date: 12 May 2010

To cite this Article Matukhina Corresponding author, Elena V. , Shchegolikhina, Olga I. , Molodtsova, Yulia A. , Pozdniakova, Yulia A. , Lyssenko, Konstantin A. , Vasil'ev, Viktor G. , Buzin, Mikhail I. and Katsoulis, Dimitris E.(2004) 'New mesomorphic organocyclosiloxanes II. Thermal behaviour and mesophase structure of organocyclohexasiloxanes', Liquid Crystals, 31: 3, 401 — 420
To link to this Article: DOI: 10.1080/02678290410001665986
URL: http://dx.doi.org/10.1080/02678290410001665986

LIQUID CRYSTALS, VOL. 31, NO. 3, MARCH 2004, 401–420

New mesomorphic organocyclosiloxanes II. Thermal behaviour and mesophase structure of organocyclohexasiloxanes†

ELENA V. MATUKHINA*

Department of Physics, Moscow State Pedagogical University, Malaya Pirogovskaya St. 1, Moscow 119882, Russia

OLGA I. SHCHEGOLIKHINA, YULIA A. MOLODTSOVA, YULIA A. POZDNIAKOVA, KONSTANTIN A. LYSSENKO, VIKTOR G. VASIL'EV, MIKHAIL I. BUZIN

Institute of Organoelement Compounds, Russian Academy of Sciences, Vavilov St. 28, Moscow 119991, Russia

and DIMITRIS E. KATSOULIS

Dow Corning Corporation, Midland MI 48686, USA

(*Received 14 July 2003; in final form 26 November 2003; accepted 1 December 2003*)

Investigations of thermotropic phase transitions performed on organocyclosiloxanes $[PhSi(O)OSiR]_6$, where R is Me_3, $Me_2(CH_2Cl)$ or $Me_2(CH{=}CH_2)$, have revealed that all these hexamers are mesomorphic compounds. The hexamers exhibit uncommon poly-mesomorphic behaviour forming two quite different mesomorphic structures. The molecular arrangement in the low temperature (LT) modification is characterized by two-dimensional (2D) long-range order with hexagonal packing. The X-ray diffraction pattern and peculiarities of molecular packing in the crystal lead us to suggest that the LT-mesophase is columnar, presumably of the Col_{hd} type. The LT-mesophase is formed by dimeric moieties, which associate with each other in column-like substructures, the ring planes not orthogonal to the stack axis. The high temperature (HT) mesophase is a plastic crystal (3D-order), where molecules take up positions in a face-centred cubic lattice. This is a very uncommon example of thermal behaviour for plastic crystals that provides a unique opportunity to bridge the gap between plastic crystalline and liquid crystalline mesomorphic behaviour. The thermal and structural properties of the mesophases depend upon the type of side groups of the hexamers. The size of the ring also affects the phase behaviour and the mesomorphic structure. This conclusion is consistent with data obtained by us earlier for cyclotetrasiloxanes.

1. Introduction

The present work is part of our study on cyclic organosiloxanes (CSs) that focuses on their mesomorphic behaviour as it relates to the chemical structure of the siloxane ring and the substituent groups on the silicon atoms. Clear information concerning the purpose of our investigation and a rationale for why the cyclosiloxanes are of interest has been presented in the first article of this series [1]. We described the mesophase ordering of cyclic organosiloxanes as the side groups and the ring size are changed independently, in order to establish their specific role in this process.

In the previous paper [1] we described results concerning thermotropic transitions in a series of organocyclotetrasiloxanes including octaphenylcyclotetrasiloxane (OPCTS).

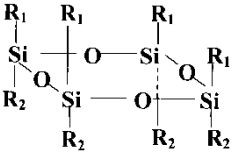

OPCTS $R_1 = Ph$, $R_2 = Ph$
I $R_1 = Ph$, $R_2 = OSiMe_3$
Ia $R_1 = Ph$, $R_2 = OSiMe_2(CH_2Cl)$
Ib $R_1 = Ph$, $R_2 = OSiMe_2(CH{=}CH_2)$
Ic $R_1 = OC_6H_4Cl$, $R_2 = SiMe_3$

*Author for correspondence; e-mail: lmatukh@mail.ru

† For part I see reference [1].

Liquid Crystals ISSN 0267-8292 print/ISSN 1366-5855 online © 2004 Taylor & Francis Ltd
http://www.tandf.co.uk/journals
DOI: 10.1080/02678290410001665986

Our results suggested that a plastic crystalline (3D) mesophase was realized in these compounds. By varying the structure of side groups attached to the silicon atoms we investigated how the substituent type influences the thermal and structural properties of the 3D-mesophase. We found that the geometry and chemical structure of side groups have a distinct influence on the mesomorphic properties of cyclotetrasiloxanes. In continuation of our investigation on cyclosiloxanes, we now report on a series of organocyclohexasiloxanes (CHSs).

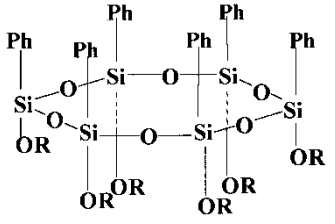

II $R = SiMe_3$
IIa $R = SiMe_2(CH_2Cl)$
IIb
$R = SiMe_2(CH=CH_2)$

For the synthesis of hexa[(phenyl)(triorganylsiloxy)]-cyclohexasiloxanes we used cage-like nickel/sodium phenylmetallasiloxane, $\{Na_2[(PhSiO_2)_6Ni_4Na_4(\mu_3\text{-}OH)_2\text{-}(PhSiO_2)_6]\}^*(L)_x$ ($L = Bu^nOH$, H_2O) (**A**). This compound, which we previously reported [2 *a*], represents a three-dimensional supramolecule, that contains two stereoregular cyclosiloxanes, *cis*-$[PhSi(O)O^-]_6$, that surround up to four transition and four sodium metal atoms to form a cage-like structure. The cyclohexasiloxanes were synthesized by two routes in accordance with the scheme: (a) the reaction of nickel/sodium phenylmetallasiloxane (**A**) with a dilute solution of hydrochloric acid giving stereoregular hexasilanol *cis*-$[PhSi(O)OH]_6$ and its subsequent treatment with triorganylchlorosilanes [2 *b*], or (b) the direct interaction of **A** with the corresponding triorganylchlorosilane. The compounds were obtained in high yield.

The compositions and structures of the resulting cyclic compounds were confirmed by elemental analysis,

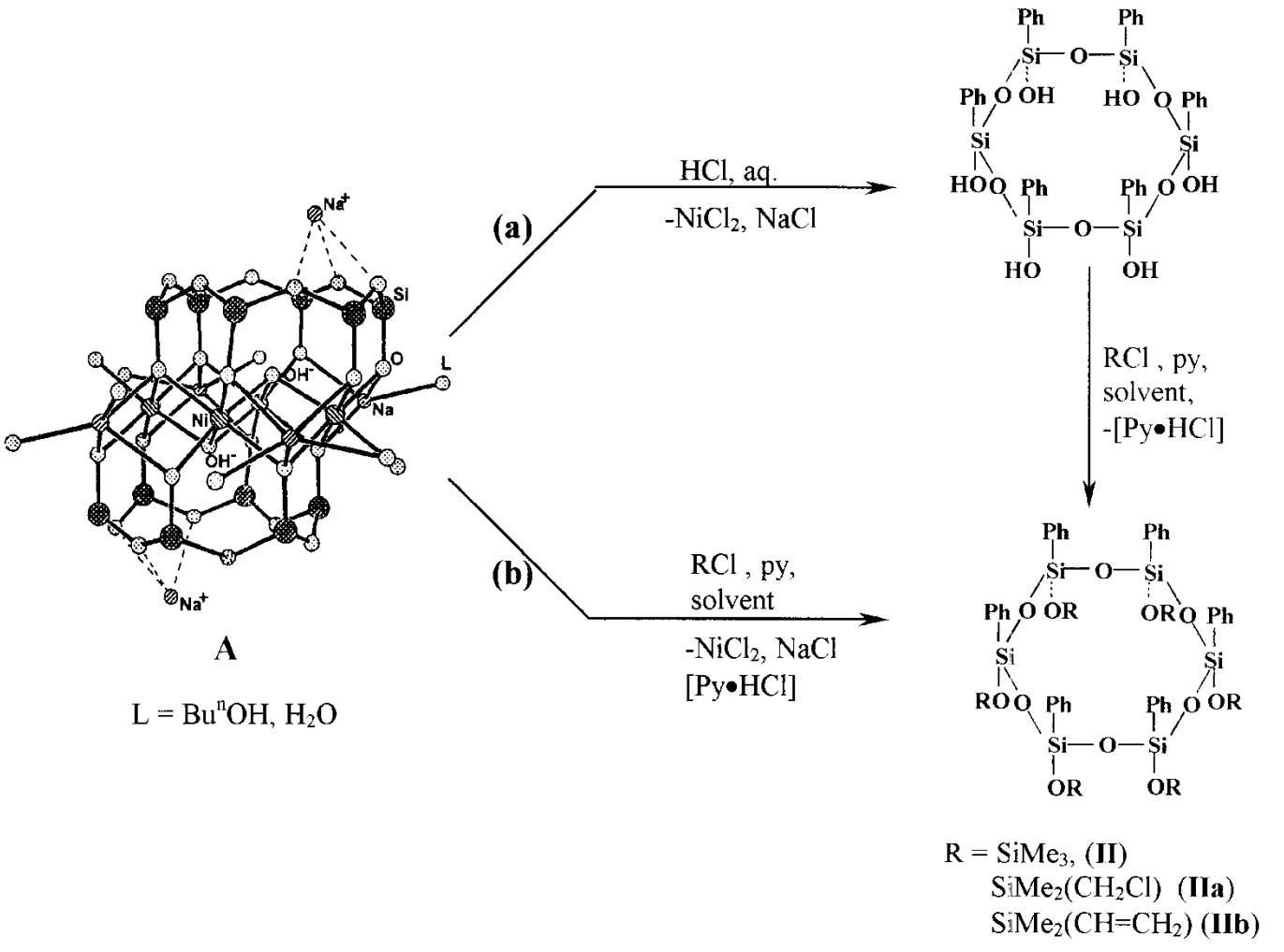

Scheme.

gel penetration chromatography and NMR spectroscopy. Additionally, the molecular structures of **II** and **IIa** were confirmed by single crystal X-ray analysis; see reference [3] and the Appendix, respectively.

2. Experimental

2.1. *Materials*

2.1.1. *Synthesis of nickel/sodium phenylmetallasiloxane (**A**)*

Phenyltri(*n*-butoxy)silane (12.80 g, 0.039 mol) and NaOH (1.80 g, 0.045 mol) were heated for 1 h under reflux in 130 ml of *n*-butanol containing 0.70 ml (0.039 mol) of water. $[Ni(NH_3)_6]Cl_2$ (3.01 g, 0.013 mol) was added to the reaction mixture, which was heated under reflux for another 2 h and the hot solution was filtered to remove NaCl. Orange crystals precipitated after partial removal of *n*-butanol and overnight storage at room temperature. After separation they were dried in vacuum at 80–90°C; yield 5.44 g (71.8%). Analysis: calcd for $\{[(C_6H_5SiO_2)_6]_2Ni_4Na_4(NaOH)_2\}(n\text{-}C_4H_9OH)_3(H_2O)_3$, $C_{84}H_{98}Na_6Ni_4O_{32}Si_{12}$, C 43.31, H 4.24, Si 14.47, Ni 10.08, Na 5.92; found, C 43,98, H 4.44, Si 14.89, Ni 9.46, Na 5.45%.

2.1.2. *Synthesis of cis-hexaphenylhexakis(trimethylsiloxy)-cyclohexasiloxane (**II**)*

The synthesis and characterization of **II** and the characteristics of its molecular structure are presented in [3].

2.1.3. *Synthesis of cis-hexaphenylhexakis[(dimethyl)(chloromethyl)siloxy]cyclohexasiloxane (**IIa**)*

A flask was charged with $Me_2(CH_2Cl)SiCl$ (25.97 g, 0.1815 mol) and pyridine (10.77 g, 0.1361 mol) in 65 ml of toluene, and 6.65 g (0.0028 mol) of **A** was added in one portion. The resulting reaction mass was stirred under reflux for 1 h. After cooling to room temperature, the precipitate was filtered off and the filtrate washed with water until a neutral Cl^- ion test with $AgNO_3$ was obtained. The organic phase was dried over sodium sulphate. The toluene was removed under vacuum, and the residue recrystallized from hot ethanol to give 8.1 g (86.1%) of white crystals. Analysis: calcd for $[C_6H_5Si(O)OSi(CH_3)_2CH_2Cl]_6$, $C_{54}H_{78}Si_{12}Cl_6O_{12}$, C 44.12, H 5.35, Si 22.94, Cl 14.48; found, C 45.11, H 5.80, Si 22.33, Cl 14.22%. ^{1}H NMR ($CDCl_3$) δ 0.39 ppm (s, Me), 2.82 (s, CH_2Cl), 6.85–7.45 (m, Ph) ^{29}Si NMR ($CDCl_3$) 5.00 ($OSiMe_2CH_2Cl$), −80.40 (O_3SiPh).

2.1.4. *Synthesis of cis-hexaphenylhexakis[(dimethyl)(vinyl)siloxy]cyclohexasiloxane (**IIb**)*

Compound **A** (5 g, 0.0021 mol) was added to a mixture of 26.58 g (0.22 mol) of $Me_2(CH_2{=}CH)SiCl$, 14.87 g (0.188 m) pyridine and dry toluene (100 ml) at room temperature and the mixture vigorously stirred, then heated under reflux for 1 h. After the mixture was cooling to room temperature, the mixture was washed free from chloride ion with water and dried over anhydrous Na_2SO_4. A white wax-like product (5.81 g) was obtained after removing the solvent and drying in vacuum (1 mm Hg/80°C/1 h). Crystallization of the product from hot methanol gave 4.54 g (74.1%) of **IIb**. Analysis: calcd for $[C_6H_5Si(O)OSi(CH_3)_2CH{=}CH_2]_6$, $C_{60}H_{84}Si_{12}O_{12}$, C 53.98, H 6.34, Si 25.27; found, C 54.49, H 6.46, Si 24.93%. ^{1}H NMR ($CDCl_3$) δ 0.24 ppm (s, Me), 5.59–6.28 (m, $CH{=}CH_2$), 6.89–7.87 (m, Ph). ^{29}Si NMR ($CDCl_3$) −1.50 ppm [$OSiMe_2CH{=}CH_2$], δ −80.44 ppm (O_3SiPh).

2.2. *Characterization*

^{1}H and ^{29}Si NMR spectra were obtained, respectively, on a Bruker DRX-500 spectrometer operating at 500 MHz and at 99.325 MHz at 20°C in $CDCl_3$. Chemical shifts are reported relative to TMS as the internal reference standard.

The thermal characteristics were read from calorimetric curves recorded on a Mettler TA-400 with DSC-30 heating attachment at a heating rate of 10 K min^{-1}. The sublimation temperatures were established by thermogravimetric analysis (TGA) using a Derivatograph-K (MOM, Hungary). TGA measurements were carried out in an air environment, using a sample size of 20–30 mg and a heating rate of 5 K min^{-1}. The temperature at which a weight loss of 1% was detected was considered as the temperature of the start of the sublimation process.

Oriented samples of the hexamers (extrudates) were obtained with a capillary rheometer at temperatures slightly higher than the melting point of the crystalline phase. The diameter of the capillary was 0.7 mm, its length was 7 mm.

The X-ray procedure was performed with filtered CuK_α radiation using a DRON-3M X-ray diffractometer with an asymmetric focusing monochromator (a bent quartz crystal), equipped with a temperature regulated heating and cooling camera. X-ray diffraction (XRD) patterns were measured over a wide temperature range, and phase diagrams were deduced from these diffraction patterns. During each experiment the temperature throughout the sample was controlled to better than 1°C. Flat camera X-ray patterns of extrudates were obtained using an IRIS-3.0 apparatus (filtered CuK_α radiation).

The assignments of transition temperatures were confirmed by polarizing microscopy. Optical birefringence studies were performed using a temperature programmable hot stage. Mettler Toledo FP-82HT

attached to a Polam L-312 microscope with crossed polarizers.

3. Phase transition behaviour

Figure 1 shows the DSC scans of **II**, **IIa** and **IIb** in sequential heating and cooling cycles; thermal characteristics of the CHSs are given in table 1.

The specific heat curves for **II** reveal two completely reversible transitions above room temperature. The transitions display considerable hysteresis and on cooling they occur at temperatures 40–50°C lower than those obtained on heating. As follows from the X-ray data presented in figure 2, the first thermal endo-effect at 55°C can be clearly attributed to the 'crystal →mesophase' transition, and the second high temperature endo-effect to the transition between two mesomorphic modifications.

The XRD patterns observed in the temperature region below 60°C (figure 2, curve A) display numerous Bragg reflections that indicate a crystal structure identical to that of the monoclinic form obtained for **II** by X-ray single crystal analysis [3]. The XRD patterns are drastically simplified above the transition, which takes place over a wide temperature range 58–80°C. The pattern obtained at 80°C, figure 2 (*b*), exhibits characteristic features of a mesophase; only three diffraction peaks and an amorphous halo are seen. Reflection intensities fall rapidly with increasing Bragg angle. The width of the first mesophase peak at half-height $\Delta_{1/2} = 0.20°$ is similar to those found for a crystalline phase. The dimensions of the mesomorphic domains are comparable with the crystallite sizes.

During the cooling process, the mesophase remains

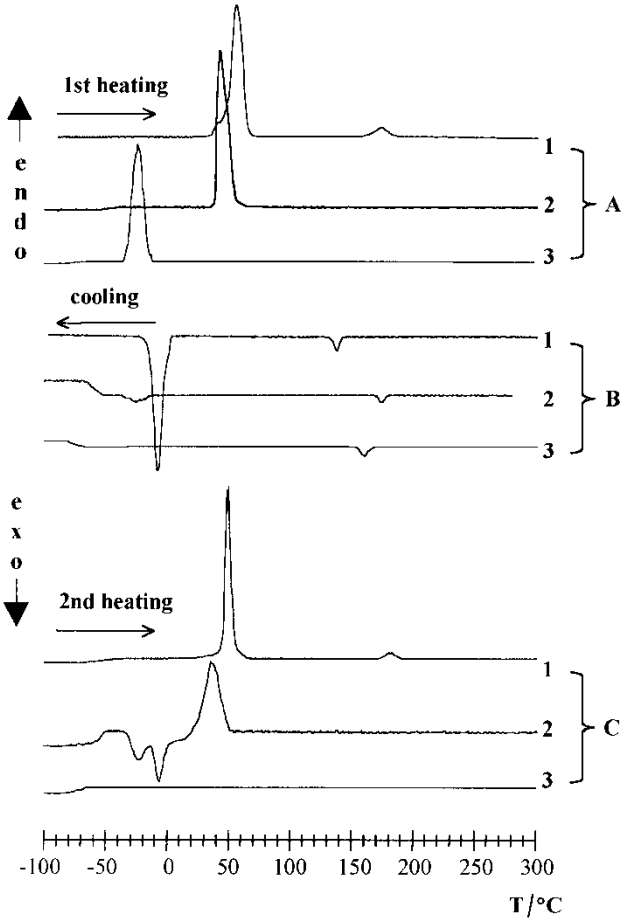

Figure 1. DSC curves for compounds **II** (1), **IIa** (2) and **IIb** (3) first heating (set A), cooling (set B), second heating (set C). Scan speed 10 K min^{-1} (c.f. table 1). All DSC curves are on the same temperature scale; the vertical scale is in W g^{-1}.

Table 1. Thermal characteristics of the organocyclohexasiloxanes **II** $R_1 = Ph$, $R_2 = OSiMe_3$, **IIa** $R_1 = Ph$, $R_2 = OSiMe_2(CH_2Cl)$, **IIb** $R_1 = Ph$, $R_2 = OSiMe_2(CH=CH_2)$.

	DSC								TGA
	Cold crystallization				crystal ↓↑ mesophase		LT-mesoph ↓↑ HI-mesoph		
Compound	Mode[a]	T_g/°C	ΔT_{ccr}/°C	ΔH/J g^{-1}	T_{mLT}/°C	ΔH/J g^{-1}	T_{mHT}/°C	ΔH/J g^{-1}	Sublimation[b] T_b/°C
II	A				55	28.9	174	2.1	240
	B				−7.4	22.9	138	1.9	
	C				49	23.7	183	1.6	
IIa	A				43	21.3			
	B	−60					175	1.2	250
	C	−54	−30–0	6.4	33	14.0			
IIb	A	−70			−8	12.0			[c]
	B	−75					159	2.7	
	C	−70							

[a]A = First heating, B = cooling, C = second heating.
[b]The temperature at which a weight loss of 1% was detected. The substances sublime directly without isotropization.
[c]The substance crosslinks without isotropization or sublimation. A weight loss of 1% was detected at 310°C.

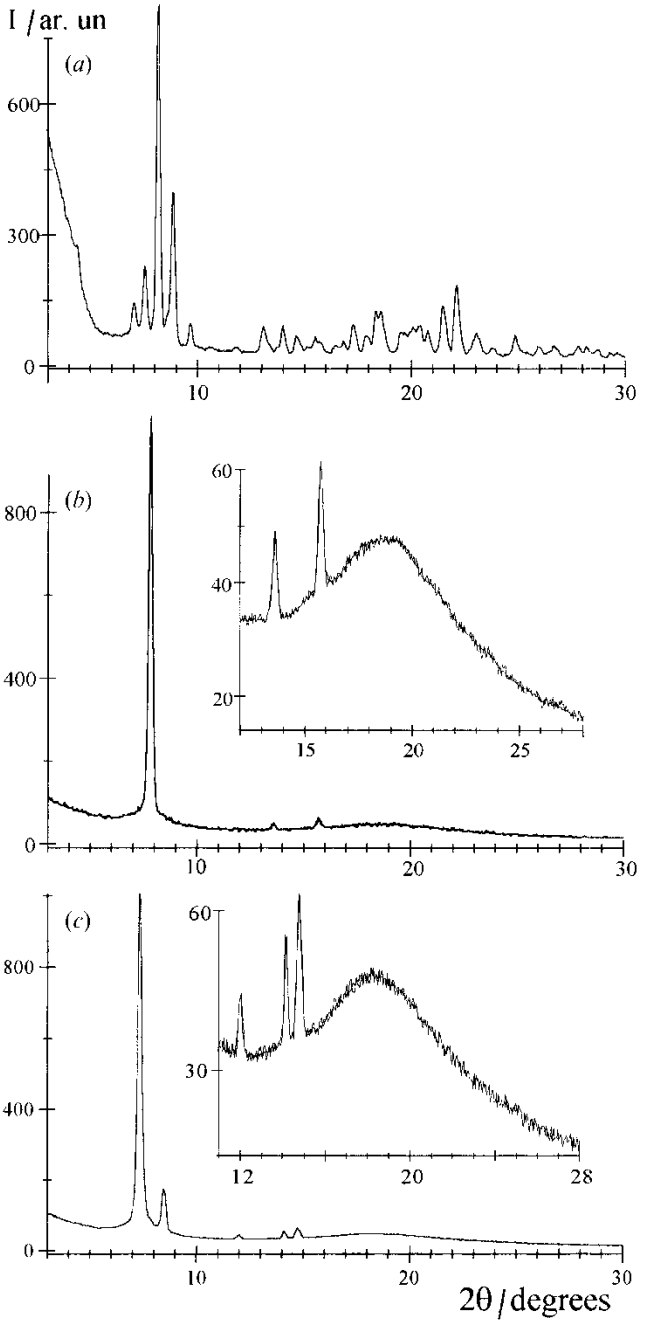

Figure 2. X-ray diffraction patterns of **II** at (*a*) 20°C, (*b*) 59°C and (*c*) 193°C.

stable to 25°C, at which point crystallization takes place. The supercooled mesophase also presents only three Bragg peaks. The values of $\sin^2\theta$ for the mesophase peaks are in the ratio 1:3:4. This ratio appears to be constant up to 158°C, but the situation changes at 160–190°C. While retaining the characteristic features of a mesophase, the X-ray pattern observed at 190°C reveals another set of Bragg peaks, figure 2 (*c*). The second endothermic peak observed in the DSC scans at 170°C may be attributed to the transition between two mesophase modifications, a low temperature (LT) and a high temperature (HT) modification. Since the Bragg peaks do not appear to become broader in the region of the polymesomorphic transition, the long-range correlation in the positions of molecular centres of mass is maintained in the HT-mesophase.

Figure 3 shows clearly the development of the polymesomorphic transition between 160 and 190°C, the XRD patterns indicating the coexistence of two mesophase modifications in a sufficiently wide temperature range. At 191°C the hexamer **II** transforms completely to the HT-mesomorphic modification form. The values of $\sin^2\theta$ for the peaks of the HT-mesophase are in the ratio 3:4:8:11:12, this ratio remaining unchanged up to 300°C. The transition to the isotropic liquid cannot be detected because the hexamer sublimes above 240°C. DSC revealed no peaks at temperatures above the polymesomorphic transition that could be reliably separated from the background noise.

Considering the DSC data obtained for CHSs containing functional groups, i.e. **IIa** and **IIb** (figure 1, table I), one can see essential changes in their thermal behaviour after the incorporation of chlorine atoms or vinyl groups in the triorganylsiloxy side exterior. The first heating scans for **IIa** and **IIb** reveal only one transition, at about 43 and −8°C, respectively. The cooling curves indicate the existence of a second high temperature transition with a small ΔH at 175 and 159°C for **IIa** and **IIb**, respectively. A slight rise of the base line in the low temperature region suggests that below −70°C the sample sets into a glassy state, partially for **IIa** or completely for **IIb** (the slight exothermic effect below 55°C was seen only on the cooling scan of **IIa**). The second heating scans of **IIa** and **IIb** are different: the exothermic peaks of **IIa** were observed just above the glass transition, indicating that an ordered structure was formed. Further heating revealed only one melting peak. On the second heating of **IIb**, only its glass transition was observed.

According to the X-ray data shown in figures 4 and 5, the first endothermic peaks correspond to the transition from a crystalline to a mesomorphic state with structure identical to that found for the LT-mesophase of **II**. On further heating the XRD patterns reveal additional Bragg peaks of the HT-mesophase at 175°C for **IIb** and at 198°C for **IIa**. However, in contrast to **II**, the coexistence of the two mesophase modifications (LT and HT) can be observed up to 285 and 260°C for **IIa** and **IIb**, respectively. This explains the lack of a detectable thermal effect in the DSC heating scans of these compounds in the temperature region of the polymesomorphic transition.

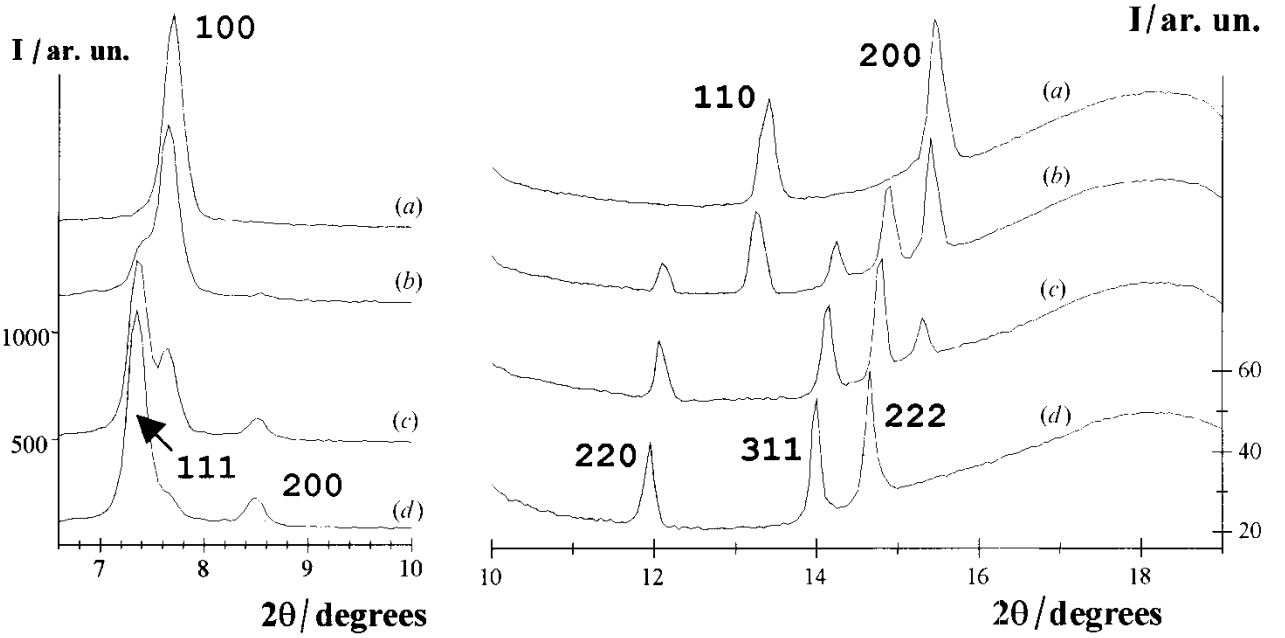

Figure 3. X-ray patterns of **II** obtained in the temperature region of the polymesomorphic transition at (*a*) 136°C, (*b*) 159°C, (*c*) 182°C and (*d*) 191°C. Note the two different scales on the intensity axis within the sections A and B. Curves (*a*) correspond to the low temperature 2D-mesophase with hexagonal lattice; the Bragg peaks observed are attributed to d_{100}, d_{111} and d_{200} spacings. Curves (*d*) correspond to the high temperature 3D-mesophase with face-centred cubic unit cell; the Bragg peaks observed are attributed to d_{111}, d_{200}, d_{220}, d_{311} and d_{222} spacings. Curves (*b*) and (*c*) represent the coexistence of the two mesomorphic modifications from 140 to 189°C.

According to the TGA data, compound **IIb** undergoes crosslinking above 260°C (table 1). There is no evidence of an HT-mesophase in the XRD patterns obtained for crosslinked **IIb** above 260°C, figure 5 (*d*), but the patterns reveal the preservation of the LT-mesophase. Thus, the crosslinking depresses the HT-mesophase of **IIb** with no influence on the LT-mesophase. Moreover, the crosslinked **IIb** loses the ability to crystallize, figure 5 (*g*). As a result, the temperature region of the LT-mesophase existence established for crosslinked **IIb** is substantially broader than for the initial **IIb**.

It should be noted that due to a slow rate of crystallization, the type of **IIa** and **IIb** structures below T_{mLT} may be different: crystalline, mesomorphic (LT-mesophase) or two-phase where the crystal and the LT-mesophase co-exist. The structure type and the phase content of the two-phase substance depend on quenching and annealing conditions. For example, X-ray measurements carried out for **IIb** after fast cooling below −10°C revealed no crystalline phase formation, and below −70°C the hexamer exhibited the glassy LT-mesophase. Fast heating from T_g did not promote crystallization. Cold crystallization of **IIb** can be induced near −38°C on slow heating only ($<3^\circ\,min^{-1}$).

4. Mesomorphic properties

4.1. *Type of order in the mesomorphic modifications*

4.1.1. *LT-mesophase*

The ratio 1:3:4 of the $\sin^2\theta$ values for the peaks at temperatures below the polymesomorphic transition indicates that the LT-mesophase has 2D-hexagonal symmetry. The peaks observed in the LT-mesophase can be indexed as 1 0 0, 1 1 0 and 2 0 0 reflections of a two-dimensional hexagonal lattice (figure 3).

4.1.2. *HT-mesophase*

The ratio 3:4:8:11:12 determined for the values of $\sin^2\theta$ of the HT-mesophase peaks indicates a face-centred cubic (f.c.c) unit cell; this conclusion is supported by calculations. It was shown that the packing coefficient k calculated on the assumption of f.c.c. molecular arrangement with one molecule per lattice point ($Z=4$) is the only one giving a good agreement with the real values of k for the mesomorphic

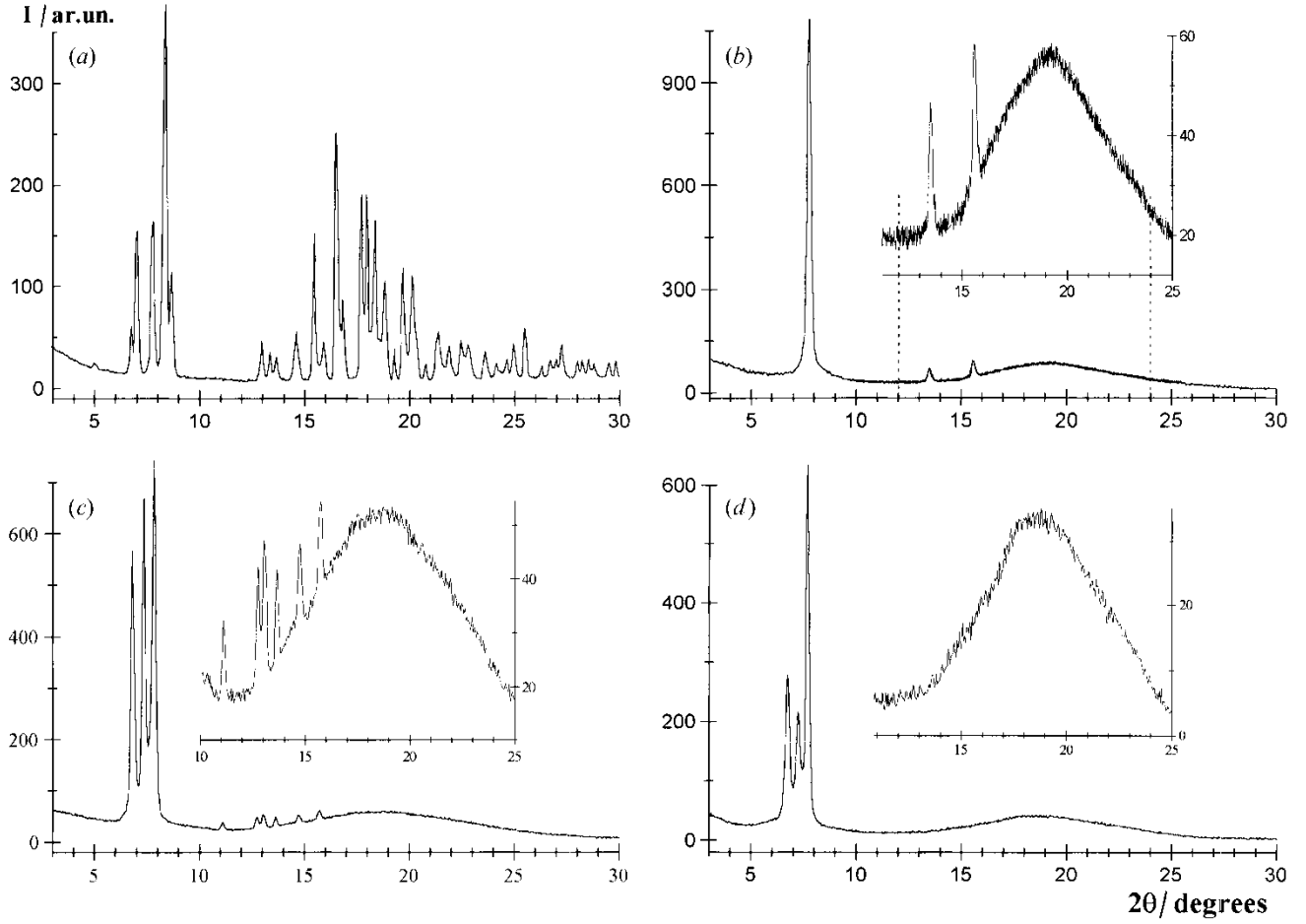

Figure 4. X-ray diffraction patterns of **IIa** at (*a*) 20, (*b*) 59, (*c*) 175 and (*d*) 280°C.

state. The peaks observed in the HT-mesophase can be indexed as 1 1 1, 2 0 0, 2 2 0, 3 1 1 and 2 2 2 reflections of a three-dimensional cubic lattice (figure 3). The ability to sublime, the optical isotropy, and the cubic unit cell of the HT-mesophase led us to the conclusion that this is an orientationally disordered 3D-mesophase (plastic crystal) [4]. It is interesting to point out that on heating within the mesomorphic state the hexamers exhibit transitions which result in an increase of the dimensionality order (2D→3D).

The asymmetric hexamer molecules must be highly disordered to form an f.c.c. lattice with one molecule per lattice point. This high crystal symmetry and the extremely rapid decrease of intensity of reflections with Bragg angle suggest randomness of molecular orientations, possibly with an average spherical symmetry. Figure 6 represents the calculated values for the parameters of the 2D-hexagonal lattice and the f.c.c. unit cell obtained for hexamer **II**. The values of a_h for **IIa** and **IIb** located below the crystallization temperature (T_{cr}) were obtained on cooling below T_{cr}.

4.2. *Molecular ordering in the LT-mesophase*

A detailed structural analysis of the LT-mesophase requires scattering experiments on macroscopically oriented samples. We were able to induce such an orientation by an extrusion of the specimens whilst in the LT-mesophase. The extrudates of **II** and **IIa**, obtained after an extrusion at elevated temperatures and subsequent cooling to room temperature, possess an oriented polycrystalline structure (figure 7). At the same time, we succeeded in obtaining oriented LT-mesophase structure at room temperature by extrusion of the hexamer **IIb**, which has the lowest temperature of 'crystal→mesophase' transition, **IIb** did not crystallize after cooling to room temperature and is transparent, in contrast to the extrudates of **II** and **IIa**. Flat camera X-ray patterns of **IIb** oriented in the LT-mesophase

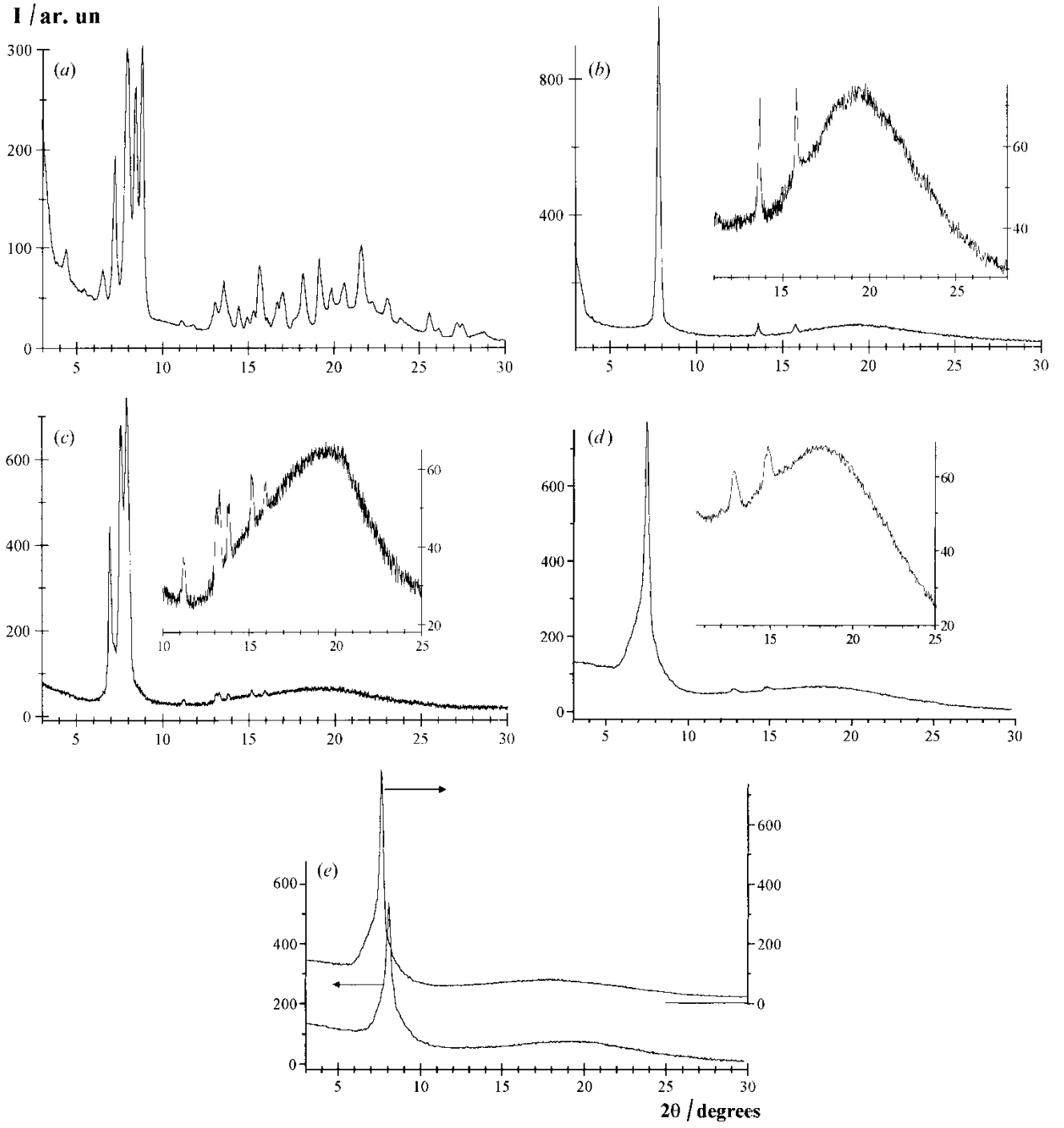

Figure 5. X-ray diffraction patterns of **IIb** obtained on heating at (*a*) −50, (*b*) 0, (*c*) 210, (*d*) 265, (*e*) 285 (upper) and −120 after cooling from 285°C (lower).

are shown in figure 8. The primary beam was either perpendicular or parallel to the extrudate long axis. The patterns are characterized by a set of reflections, which were also revealed in the XRD patterns, figure 2 (*b*), and marked as A, B, C and D in figure 8.

The pattern obtained with the primary beam being perpendicular to the long axis of the extrudate is a direct image of the reciprocal lattice of a 2D-hexagonal structure, the ordered hexagonal plane being oriented predominantly along the long axis of the extrudate, i.e. parallel to the flow direction. Therefore, the Bragg reflections A, B and C displayed in figure 8 can be

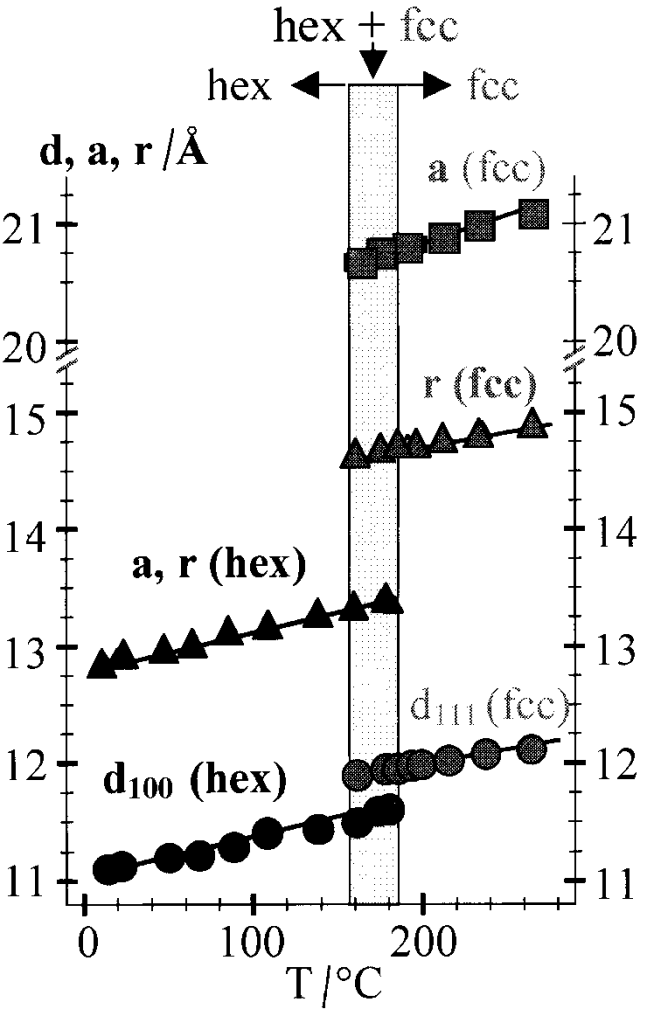

Figure 6. The effect of temperature on the structural characteristics of the mesomorphic state for compound **II**. The left-hand set shows the parameters d_{100} (●) and $a_h = r$ (▲) of the 2D-hexagonal lattice of the LT-mesophase. The right-hand set shows the parameters d_{111} (●), $r = 0.707a_c$ (▲) and a_c (■) of the f.c.c. unit cell of the HT-mesophase (r = the distance between nearest neighbouring molecules). Note the a-axis break eliminating the region with no data, and the difference in scales for the parameters a_h and a_c. The dashed area indicates the temperature region of the polymesomorphic transition.

indexed in terms of a hexagonal 2D-lattice as 1 0 0, 1 1 0 and 2 0 0 reflections. At the same time, there is no evidence of an orientation on the pattern obtained with the primary beam being parallel to the extrudate long axis; the pattern demonstrates that the scattering intensity is uniformly distributed on three circles. A diffuse ring C is observed in both patterns (as described above, there is also an amorphous halo in XRD patterns of the mesophase). This may be attributed to a non-oriented liquid-like arrangement of side groups

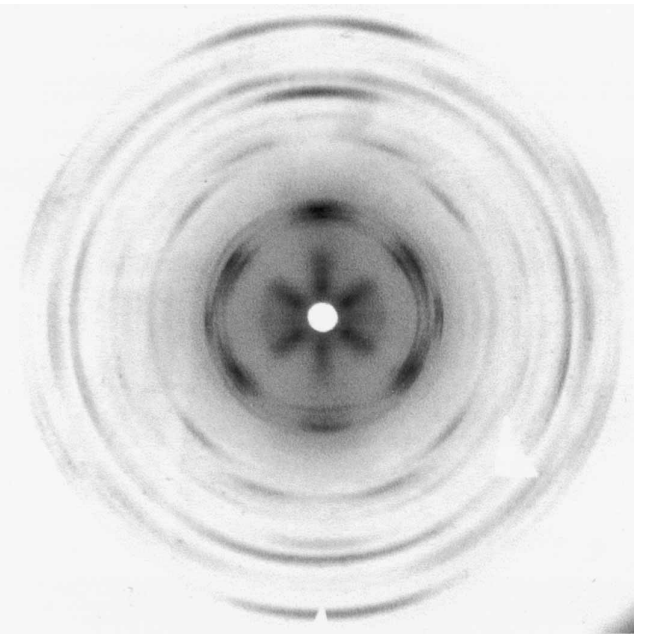

Figure 7. Flat camera X-ray pattern of the extrudate of compound **II** in the crystalline state obtained at 20°C with the primary beam perpendicular to the long axis of the extrudate.

within the macroscopically oriented sample. Based on these data we propose that the mesophase domains with 2D-hexagonal molecular packing are oriented within an extrudate as presented in figure 8 (c).

Figure 8 (a) shows the 1 0 0 reflection located on the meridian of the pattern, the corresponding molecular arrangement of the *ab* plane of a hexagonal lattice with respect to the extrudate axes is shown in figure 8 (d). The same arrangement should also be inherent to the extrudates of **II** and **IIa** in the LT-mesophase. This conclusion is based on XRD data obtained for extrudates of **II** and **IIa** upon heating. (The measurements were carried out on a specimen prepared by stacking about 20 extrudates aligned in parallel into a compact bundle.) On heating just above the temperature of the 'crystal→mesophase' transition the appearance of the 1 0 0 peak was detected by scanning in the meridian direction.

The appearance of the oriented polycrystalline structure after an extrusion at the temperature of the LT-mesophase (figure 7) indicates a strong connection between molecular ordering in the crystalline and LT-mesomorphic states. To aid the interpretation of results it is useful to refer to data from single crystal X-ray analysis of compound **II** [3] regarding molecular ordering in the mesophase. The crystallographic data obtained at −120°C for the monoclinic unit cell are $a = 20.247(7)$ Å, $b = 17.772(5)$ Å, $c = 39.755(12)$ Å,

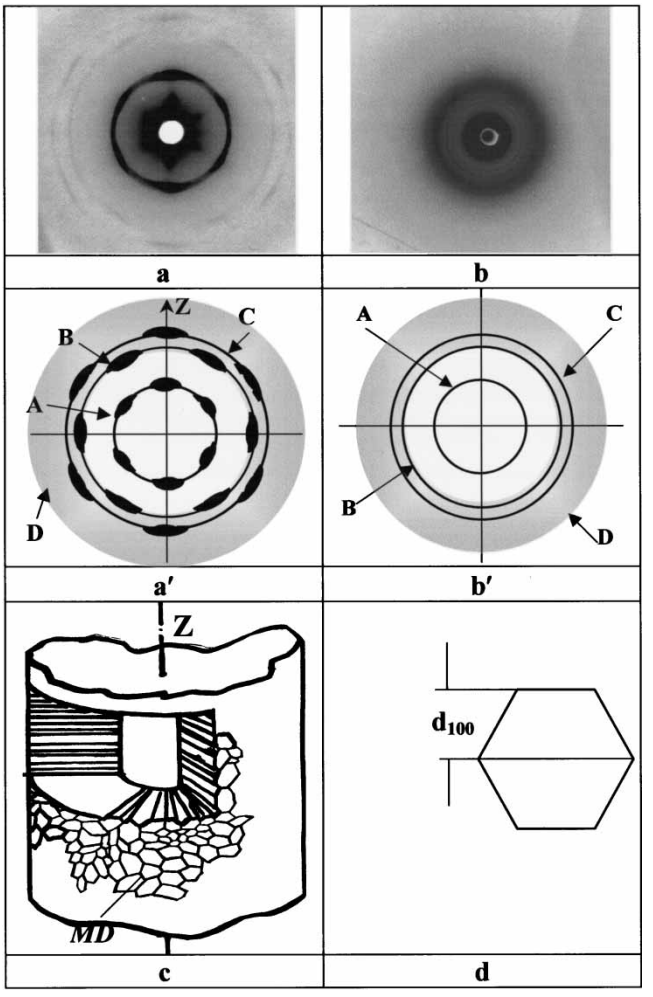

Figure 8. Flat camera X-ray patterns of the extrudate of compound **IIb** in the LT-mesophase obtained at 20°C with the primary beam perpendicular (a) and parallel (b) to the long axis **Z** of the extrudate, and their schematic representation (a′ and b′). The difference between the diameters of the diffraction circles on the patterns a and b is due to the different distances between the sample and the camera used in these experiments. The ordering possessed by LT-mesophase domains (MD) which may occur in the extrudate is shown in (c), and the arrangement of the *ab* plane of the 2D-hexagonal lattice with respect to the long axis Z of the extrudate in (d).

$\beta = 96.93(2)^\circ$, $V = 14201\,\text{Å}^3$, space group $C2/c$, $Z = 8$. The identical crystalline structure is inherent to the extrudates as well as to the initial polycrystalline powder of **II**. The molecular packing in the monoclinic crystal of **II** is presented in figures 9 and 10.

Figures 9 and 10 show that the planes of the cyclosiloxane are practically orthogonal to the *c* axis of a crystal and predominantly parallel to the *ab* crystal plane. A characteristic feature of the molecular arrangement is clearly seen in figure 9. The rings are packed together so that the Ph groups in a given ring are adjacent to Ph groups in its neighbouring rings. This aggregation comes from the bipolar nature of the molecules. There is a pronounced separation between phenyl and trimethylsiloxy groups in the crystal.

Following arguments we put forward previously during the study of tetramers [1], we propose that the transition 'crystal→mesophase' observed for **II** at T_{mLT} is related only to the increased mobility of trimethylsiloxy groups. The Ph groups are not mobile at T_{mLT}, as strong interactions between them are still present. Therefore, only a partial destruction of the crystal structure should accompany the transition to the mesophase. Hence, one may predict the appearance of substructures as the basic structural units of the LT-mesophase at T_{mLT}. As follows from figures 9 and 10, two alternative types of such noncovalent-bonded substructures can be theoretically proposed: (i) a linear double-chain polymer-like associate with long axes parallel to the *b* axis, marked S_{pdc} in figure 9, (ii) a columnar associate marked S_{col} in figure 10 (*a*), formed by dimeric moieties, figure 10 (*c*), with the stacking axis predominantly orthogonal to the *ab* plane. But only the second columnar type appears to be consistent with all the experimental data.

The diameter of the polymer-like associates S_{pdc} is close to 20 Å, i.e. to half the value of the monoclinic parameter *c*, and thus is substantially larger than parameter a_h of the LT-mesophase (figure 5). In contrast, the size of the projection of the molecule on the *ab* plane is comparable with the value of a_h, figure 10 (*b*). As follows from figure 10, the transition from crystal to mesophase should involve a slight decrease of the area per molecule in the *ab* plane, causing them to lie tilted with respect to the stack axis of mesophase columns coinciding with the *c* axis of the crystal.

These arguments are supported by the analysis of the XRD patterns of the extrudates of **II** with oriented polycrystalline structure (figure 7). The Bragg peaks at $2\theta = 8.64^\circ$, 17.33° and 26.14° located on the meridian correspond to reflections 2 0 0, 4 0 0 and 6 0 0 of the monoclinic unit cell [3]. Thus, for the majority of the crystallites the crystallographic *a*-axis is presumably oriented along the extrudate axes.

The columnar S_{col} type of proposed substructure also coincides with the data obtained for the oriented LT-mesophase (figure 8), where the *ab* plane of the hexagonal lattice is shown to be parallel to the extrudate *Z* axes. It is obvious that the extrudate obtained due to the flow of the substructures S_{pdc} shown in figure 9 must show a quite different texture, i.e. the C-texture typical for columnar polymers, where the *ab* hexagonal lattice plane is orthogonal to *Z*. The

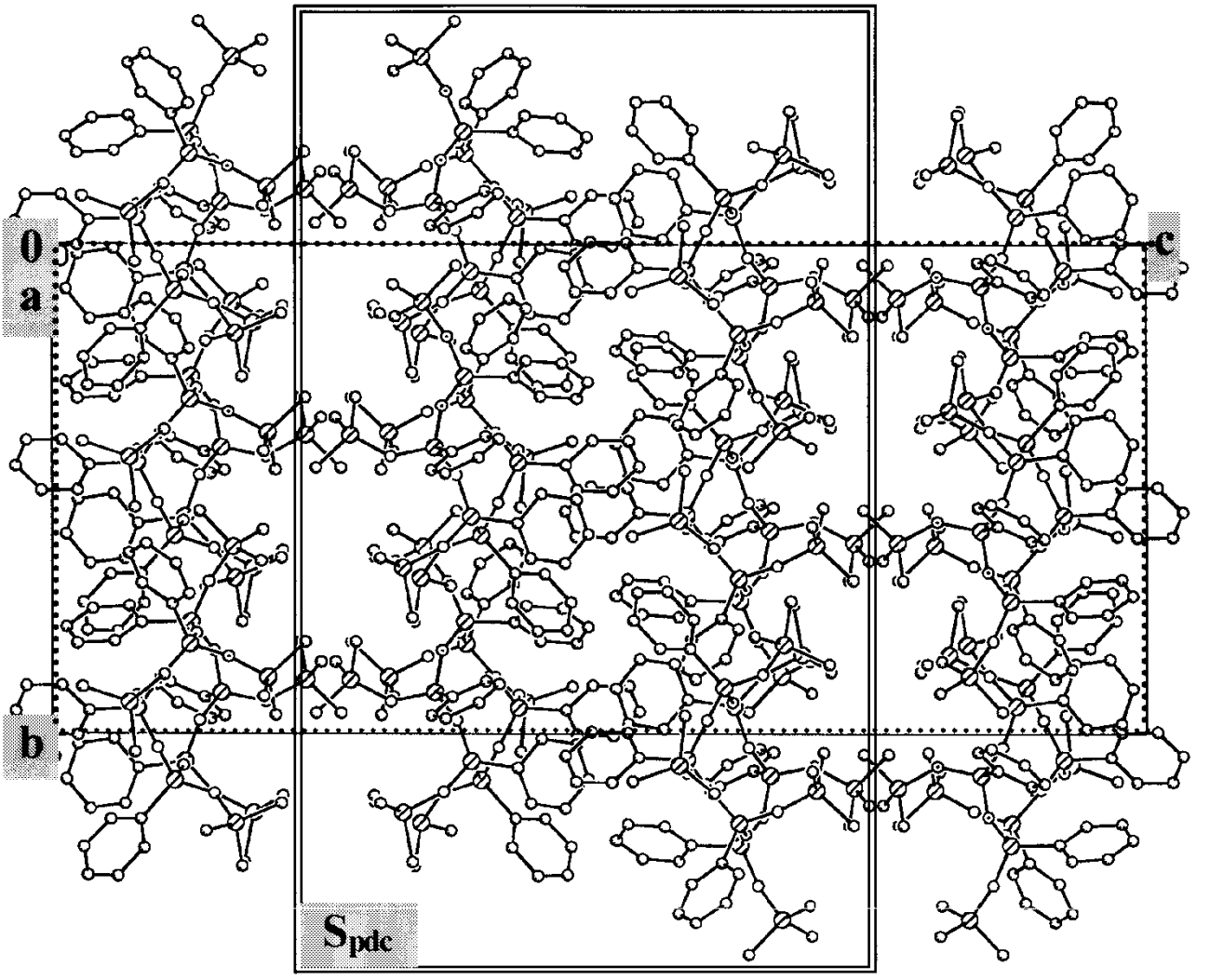

Figure 9. Molecular packing in the monoclinic crystal of compound **II** (the projection on the *bc* plane). One of the possible substructures of the LT-mesophase, a double chain polymer-like S_{pdc}, is marked out.

columnar S_{col} type of substructure can be marked on considering the molecular packing established for **IIa** by the X-ray measurements carried out for a single crystal (figure 11) (crystallographic data for **IIa** are presented in the Appendix).

All these data as well as the six-fold symmetry of CHS molecules support our hypothesis that the LT-mesophases of all the hexamers under study belong to Col_{hd}-type columnar structures. However, we did not succeed in finding additional confirmation of this supposition. First, attempts to obtain optical textures using crossed polarizers were unsuccessful. The lack of birefringence in the temperature region of the LT-mesophase was established not only on bulk samples but also on a thin slice of an oriented extrudate of **IIb** (figure 8) with varying orientation of the flat surface with respect to the ordered 2D-hexagonal plane. However, the CHSs LT-mesophase was less transparent than the isotropic phase and it was possible to observe it in ordinary light. Secondly, attempts were made to carry out a miscibility study with benzene hexa-*n*-heptonate as a standard reference discotic material, but these were also unsuccessful. The two specimens appeared to be immiscible.

Despite the fact that the scattering patterns of the LT-mesophase and the columnar 2D-mesophase Col_{hd} are very similar, one may suppose that the possibility exists for other quite different packing in the LT-mesophase. First, a plastically crystalline mesophase with hexagonal packing can be assumed, such as that of some plastic crystals—although hexagonal packing has very rarely been observed [4, 5]. One of these, norborane, undergoes a thermotropic transition to a high temperature mesophase with an f.c.c. lattice [6].

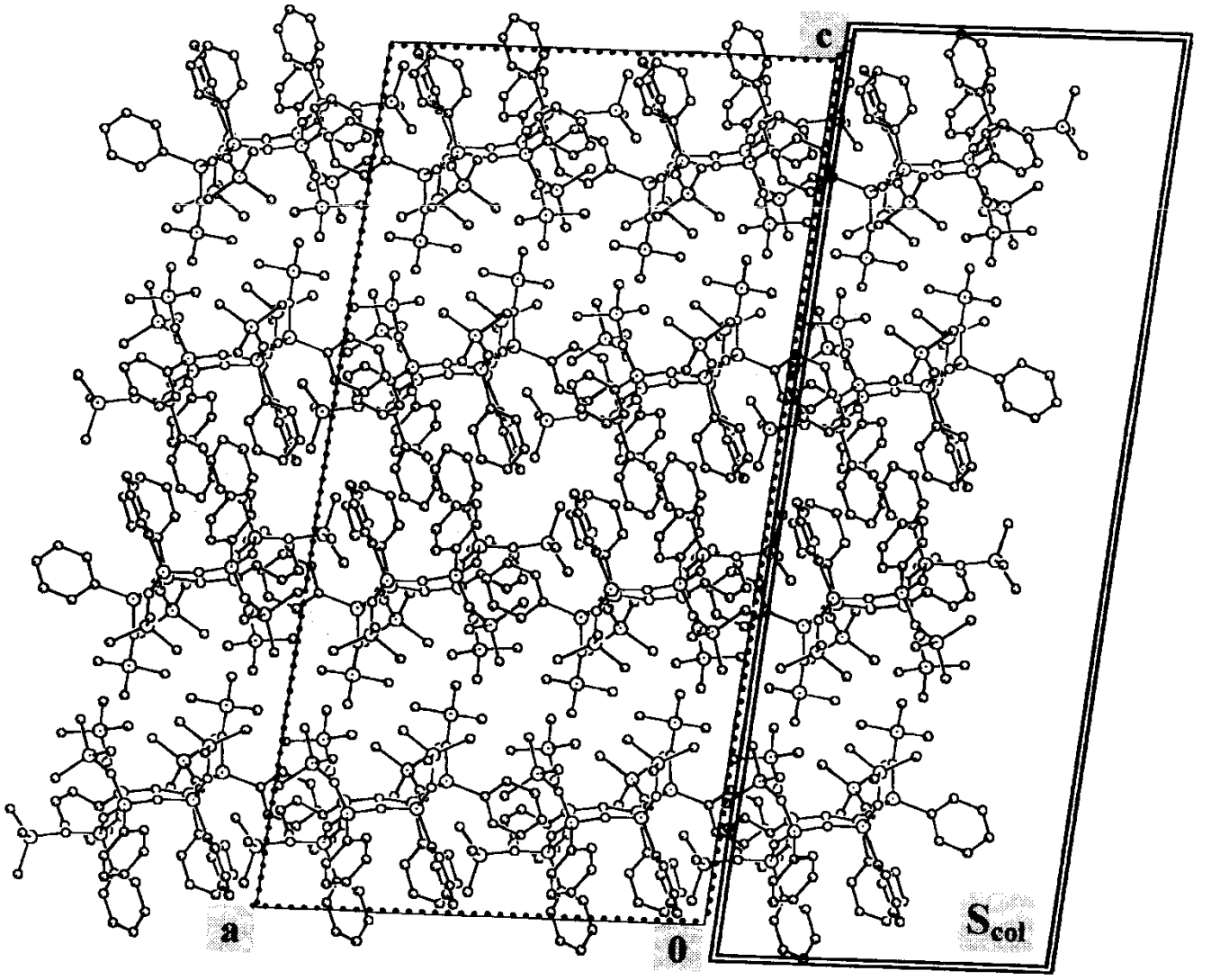

(*a*)

Figure 10. The molecular packing in the monoclinic crystal of compound **II** (*a*) The projection on the *ac* plane. One of the possible substructures of the LT-mesophase, a columnar-like S_{col}, is marked out. It is clearly seen that trimethylsiloxy and Ph groups are oriented in different directions with respect to the *ab* plane. (*b*) The projection on the *ab* plane. (*c*) Non-covalent bonded dimeric moiety, which we suggest is the basic structural unit of the LT-mesophase. *Continued.*

However, here we should mention that all plastic crystals with hexagonal packing are characterized by h.c.p. (hexagonal closed packed) lattices with a bimolecular unit cell and a *c*/*a* ratio of 1.60 (*a* and *c* are parameters of the hexagonal unit cell). As to the hexamer under study, the peaks observed in the scattering pattern of the LT-mesophase cannot be indexed on the assumption of an h.c.p. molecular arrangement.

Moreover, the molecular arrangement in the LT-mesophase cannot even be considered as a 'distorted' h.c.p. lattice with a bimolecular unit cell and a *c*/*a* ratio slightly different from 1.60. This conclusion results from the following considerations. The X-ray data for the LT-mesophase suggest the existence of a long-range order in two dimensions only, i.e. in the plane perpendicular to the *c* axis of the hexagonal lattice. It is possible to state approximately the value of the average periodicity in the third direction, i.e. the distance between the nearest neighbouring molecules c^{av} along the *c* axis of the hexagonal lattice. For the hexamers the values of *a* differ very slightly. Therefore, we will carry out our approximation for **II**, whose crystallographic data are available.

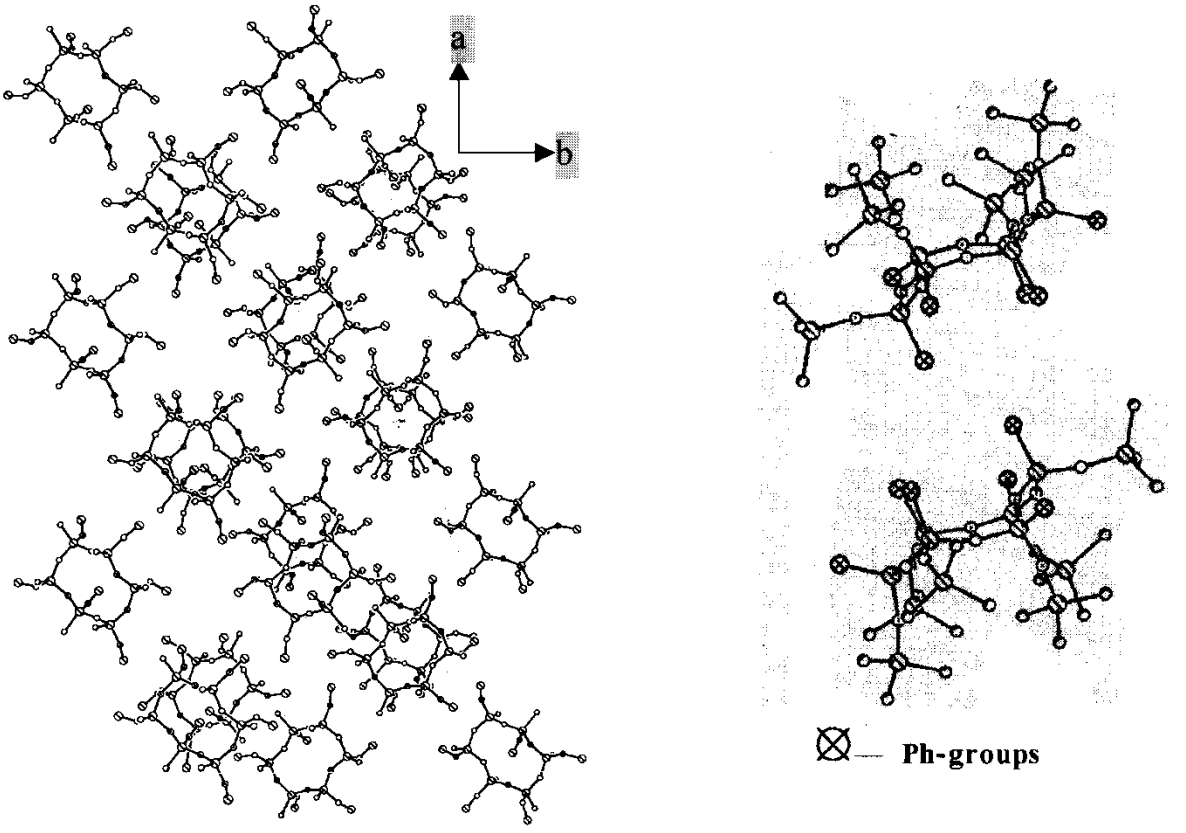

(*b*) (*c*)

Figure 10 *continued.* (*b*) and (*c*)

In a crystal of **II** the packing coefficient k [7] is very small $k=0.679$ at -120°C. At the same time, the temperature interval of the mesophase existence is very broad. Hence, we can assume that the value of k in the LT-mesophase does not differ substantially from 0.68 at temperatures just near the melting of the crystal. Then, the value of c^{av} for supercooled mesophase at 12°C is close to 12.4 Å, as the parameter of the 2D-hexagonal lattice $a=12.85$ Å and $\Sigma\Delta V_i \sim 1205.04$ Å^3. ($\Sigma\Delta V_i$ is the sum of the van der Waals volumes calculated for the increments of the atoms forming a molecule [7].) Hence, the distances between the nearest neighbouring molecules in the ordered plane (12.85 Å) and along the axis orthogonal to this plane ($\sim$12.40 Å) differ very slightly. Moreover, the calculated value of c^{av} differs significantly from the value that must be observed for an h.c.p. lattice ($Z=2$), where $c/a=1.60$. Indeed, for an h.c.p. lattice, if $a=12.85$ Å, then $c=20.56$ Å and $c^{av}=10.28$ Å, with $k=0.82$ at 12°C.

There is a way to assess this result further. Figure 6 shows that there is a temperature region of coexistence of two mesophase modifications. Based upon the assumption that in this very temperature region the values of the packing coefficient k for both modifications differ slightly, one can calculate approximately the average periodicity along c^{av} for this temperature interval. The calculated value is 14.14 Å, quite different from the c^{av} value, which should be observed for an h.c.p. lattice, where if $a=13.33$ Å, then $c=21.33$ Å and $c^{av}=10.67$ Å, with $k=0.73$ at 183°C.

As follows from all the approximations carried out, the LT-mesophase ordering differs from that in the plastically crystalline state. The other argument in favour of the non-plastically crystalline nature of the LT-mesophase is based on experimental evidence obtained for cyclohexasiloxanes in the presence of impurities, which are known to suppress the plastically crystalline phase even at low concentrations [4]. We found by XRD and DSC studies that the impurities have no influence on the LT-mesophase formation but, as a natural result, suppress the cyclohexasiloxane ability to form a plastically crystalline HT-mesophase. As a result, the 2D-mesophase was observed up to the sublimation temperature. Moreover, heating **IIb** to

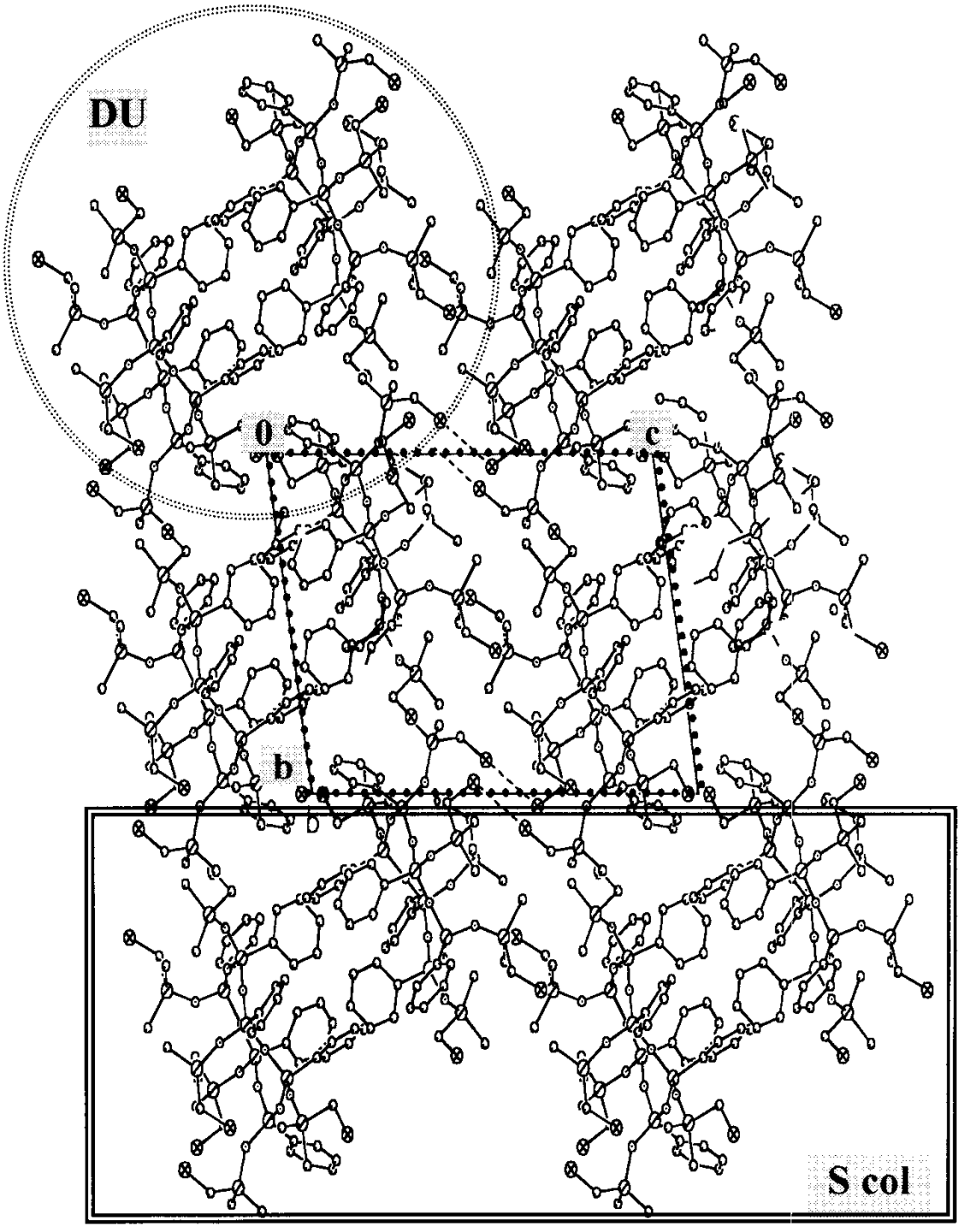

Figure 11. Molecular packing in the triclinic crystal of compound **IIa**, the projection on the *bc* plane. A columnar-like substructure S_{col} of the LT-mesophase is marked.

260°C leads to a partial crosslinking due to the presence of vinyl groups. The crosslinked hexamer loses the ability to crystallize but preserves the ability to attain mesomorphic ordering with 2D-hexagonal packing.

Taking into account all these arguments, as well as the X-ray data discussed earlier, we conclude that the LT-mesophase realized in hexamers should be attributed to the columnar Col_{hd} type. The LT-mesophase

consists of dimeric moieties, which associate with each other in column-like substructures. As follows from the X-ray data and the molecular packing in figures 10 and 11, the dimeric moieties most probably do not lie normal to the stack axis of a column. Moreover, the dimeric moieties can possess a form of oblique cylinders due to slight displacement of one ring with respect to the other, figure 10 (*c*). This molecular arrangement within columns creates favourable packing conditions for the strong interactions between Ph groups of adjacent dimeric moieties, ensuring column stability. The proposed intra-columnar packing appears to offer a convincing explanation for the experimental fact of the lack of a scattering peak corresponding to the average stacking distance of the molecules within the columns. The presence of this scattering peak is an intrinsic feature of the X-ray patterns of classical discotic mesophases. In the case of the D_{hd} type, this peak is diffuse but well defined and its appearance is caused by the presence of electron density fluctuations along columns. In our case the electron density distribution along columns with the molecular packing proposed for hexamers is expected to be smooth, agreeing with the absence of a peak associated with intracolumnar scattering on the X-ray patterns of the CHS LT-mesophase.

One central question still remains. Is the LT-mesophase of CHSs columnar or bowlic? It is well known that all bowlic mesophases found so far are columnar as in the case of discotic mesophases. However, in bowl-like molecules the up–down symmetry is broken, which distinguishes them from disk-like molecules. Based only on this molecular architecture, CHS molecules should be attributed to the class of bowlic mesogens.

4.3. *Polymesomorphism of hexamers*

Special attention should be paid to the ability of CHS molecules to form two quite different mesomorphic structures. This is an unusual phenomenon since it is well known that each type of mesomorphic structure requires quite definite demands on the shape of molecules forming these structures. In other words, there exists a critical value of molecular anisotropy γ_{cr} that limits the probability of molecules to form a distinct type of mesomorphic structure. At the same time, it has been shown [8] that when the shape of molecules is close to critical, even a slight change in molecular architecture can lead to a drastic transformation of properties inherent to the mesomorphic system as a whole.

From all these arguments it follows that it must be peculiar features of the hexamer molecules that create the necessary conditions for the formation of the quite different structures within the mesomorphic state. The only possible approach to satisfy the criteria discussed above seems to be based on the assumption that the shape of CHS molecules is close to a critical one. In proposing this we follow the arguments put forward by our data for CTS forming only the 3D-mesophase [1]. The temperature region of their mesophase existence practically coincides with that for the 2D-mesophase of the hexamer. As CHS and CTS molecules differ from each other only by the size of the cyclosiloxane ring, it is apparent that the value of molecular anisotropy for the CHS molecule (the ratio between its diameter D and thickness h) is only a little larger than for the CT molecule. Indeed, the cyclic core of a siloxane tetramer is almost planar and can be approximately represented as a disk with a thickness $h_c \approx 4.2$ Å and a diameter of a circle in a foot $D_c \approx 8.6$ Å. As for the hexamer, its cyclic core can be roughly represented as a disk with $h_c \approx 4.5$ Å and a diameter of rotation about the axis perpendicular to a cyclic core equal to $D_c \approx 11.8$ Å. So, the difference in the value of molecular anisotropy (in the aspect ratio) for CTS and CHS molecules seems to be less than 28%.

Therefore, to form a 2D-mesophase the hexamer molecules must possess a shape with the anisotropy $\gamma_{2D} > \gamma_{cr}$. In view of the hexamer ability to form a 3D-mesophase at elevated temperatures the value γ_{2D} must be a little larger than γ_{cr}. Moreover, the hexamer is certain to undergo a slight alteration of molecular shape at elevated temperatures, leading to a reduction in the value of molecular anisotropy in the temperature region of the 3D-mesophase existence ($\gamma_{3D} \leqslant \gamma_{cr} < \gamma_{2D}$). In other words, the hexamer molecule, possessing a lath-like shape with a small anisotropy value below the temperature of polymesomorphic transition $T_{LT\text{-}HT}$, must take a quasi-spherical form just above $T_{LT\text{-}HT}$.

The driving forces for the thermotropic alteration of molecular shape seem to be inherent in the chemical constitution of a CHS molecule itself. Two general features of CHS molecules can obviously be regarded as most essential, namely the two types of substituents and the flexibility of the hexasiloxane ring. The presence of the two types of side groups creates conditions for the two-step thermal 'defrosting' of the side chain and rings mobility. The increase of mobility of triorganylsiloxy groups at lower temperatures leads to the transition to the LT-mesophase, where Ph groups are not yet mobile, and the strong interactions between them create the anisotropy of intermolecular forces necessary for the 2D-mesophase stability. At the same time, the interactions between Ph groups seem to prevent the conformational disordering of the hexasiloxane ring. The increasing mobility of Ph groups at

higher temperatures results in the disappearance of the anisotropy of intermolecular forces and in the conformational disordering of the ring, leading to the quasi-spherical symmetry of the CHS molecule, necessary for the formation of a 3D-plastically crystalline mesophase.

4.4. *The effect of side groups on the thermal and structural characteristics of a mesophase*

The structural organization of the mesomorphic modifications for all CHSs is alike. In the LT-mesophase, all CHSs possess an LC ordering with molecular packing identical to those of a Col_{hd}-type columnar mesophase. In the HT-mesophase, CHSs are plastic crystals with the molecular centres of gravity located in an f.c.c. unit cell. The increasing size of a CHS molecule in a range **II**→**IIb**→**IIa** ($\Sigma\Delta V_i = 1206.8$, 1280.9, 1295.9 Å^3) leads to an increase of the parameters a_h and a_c of a 2D-hexagonal lattice and an f.c.c. unit cell, as well to an increase in the distance between nearest neighbouring molecules r in the LT- and HT-mesophases ($a_h = r$ and $a_{fcc} = 0.707\ r$) (figure 12). The parameter a_c of the HT-mesophase appeared to be more sensitive to changes in the CHS molecular size. This effect can be explained by taking into account that the transition from the LT- to the HT-mesophase is accompanied by an appreciable increase in the mobility of side groups, creating sufficient free volume for a molecule to reorient within its cage. Of the hexamers described, the **IIa** molecules, which exhibit the largest f.c.c. unit cell, are characterized by the largest $\Sigma\Delta V_i$ value and by very strong interactions between chlorine atoms.

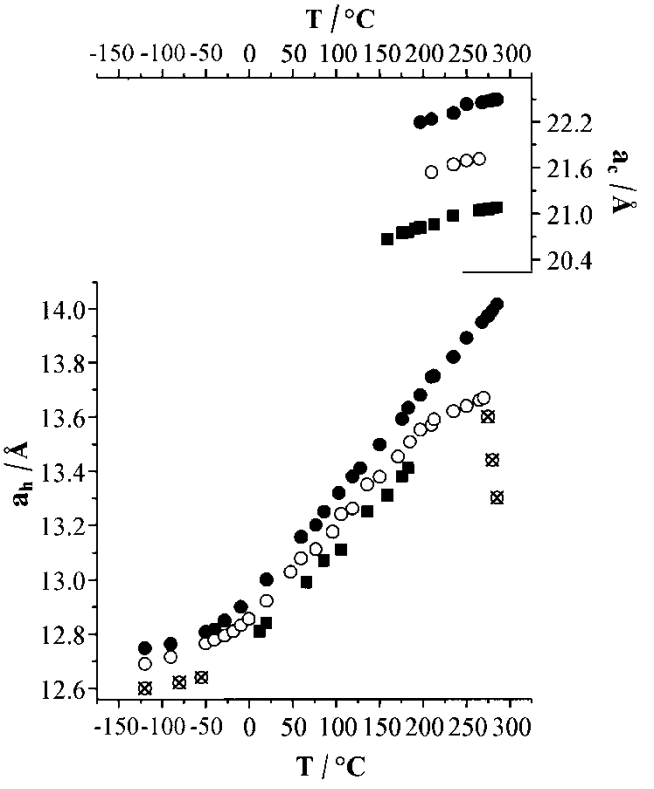

Figure 12. Temperature dependence of the parameter a_h of the 2D-hexagonal lattice of the LT-mesophase (the lower set) and the parameter a_c of the f.c.c. unit cell of the HT-mesophase (the upper set) for compounds **II** (■), **IIa** (●), **IIb** (○) and for the crosslinked compound **IIb** (⊗). Note the difference in the scales for the parameters a_h and a_c.

The presence of functional groups in **IIa** and **IIb** results in a broadening of the temperature region of the mesophase existence in comparison with **II**, owing to the shift of the crystal–mesophase transition to lower temperatures and because of the higher sublimation temperatures of **IIa** and **IIb**. The lowering of the T_{mLT} is most probably connected with crystal disturbances because of steric hindrance and strong interactions between polar and larger side groups of **IIa** and **IIb**. Apparently the same effects slow down the polymesomorphic transition. The hexamers **IIa** and **IIb** are characterized by higher temperatures of the polymesomorphic transition and by a much broader temperature region within which the LT- and HT-mesophases coexist, in comparison with **II**.

The appearance of functional groups in CHS side groups led to a substantial lowering of the crystallization rate. Using high cooling rates one can obtain mesomorphic glasses of **IIa** and **IIb** below T_g. As a result, on subsequent heating, the structure of these hexamers just below T_{mLT} depends on the heating rate. Compounds **IIa** and **IIb** can exhibit a mesophase, crystalline or two-phase (mesophase + crystal) structure. The lowest rate of crystallization is applicable to **IIb**.

This discussion indicates that the effect of the side groups on the thermal and structural characteristics of the CHS mesophase is similar to that observed for the tetramers *cis*[PhSi(O)(OSiMe$_2$*R*)]$_4$ with *R* = Me (**I**), CH_2Cl (**Ia**), $CH{=}CH_2$ (**Ib**) [1]. For the tetramers and hexamers under study, the longitudinal dimensions and the van der Waals volumes of the side groups differ only slightly. Consequently, changes in the chemical content of the CS side groups can influence only the transition temperatures and the parameters of the mesophase structure; they cannot induce any transformation of the mesophase structure. However, drastic changes in the mesophase structure can be observed on varying the CS ring size.

Table 2. The effect of the size of a siloxane ring and the chemical structure of side groups on the phase behaviour, mesophase formation and mesophase structure of *cis*-cyclosiloxanes: *cis*-{PhSi(O)[(OSi(Me)$_2$(*R*)]}$_n$ with *R* = Me, CH_2Cl, $CH=CH_2$ and *n* = 3,4,6 (transition temperature, in °C)

Compound	State: Crystal	Mesophase	Isotropic	Sublimed
Trimer	•	$\overset{59^a}{\underset{5}{\rightleftharpoons}}$	•	
Tetramers				
I	• $\overset{78}{\underset{29}{\rightleftharpoons}}$	• One modification only, 3D long range order, plastically crystalline mesophase, body-centred cubic unit cell	$\overset{262}{\underset{258}{\rightleftharpoons}}$ • $\overset{242}{\underset{b}{\rightleftharpoons}}$	•
Ia	• $\overset{45}{\underset{c}{\rightleftharpoons}}$		$\overset{c}{\underset{c}{\rightleftharpoons}}$ • $\overset{260}{\underset{b}{\rightleftharpoons}}$	•
Ib	• $\overset{31}{\underset{c}{\rightleftharpoons}}$		$\overset{273}{\underset{264}{\rightleftharpoons}}$ • $\overset{255}{\underset{b}{\rightleftharpoons}}$	•
Hexamers				
II	• $\overset{55}{\underset{-7}{\rightleftharpoons}}$	• LT-mesophase 2D long-range order, columnar Col_{hd} mesophase, flat hexagonal lattice. • $\overset{174}{\underset{138}{\rightleftharpoons}}$ HT-mesophase 3D long-range order, plastically crystalline mesophase, face-centred cubic unit cell.	$\overset{c}{\underset{c}{\rightleftharpoons}}$ $\overset{278}{\underset{b}{\rightleftharpoons}}$	•
IIa	• $\overset{43}{\underset{c}{\rightleftharpoons}}$	• $\overset{c}{\underset{175}{\rightleftharpoons}}$	$\overset{c}{\underset{c}{\rightleftharpoons}}$ $\overset{309}{\underset{b}{\rightleftharpoons}}$	•
IIb	• $\overset{-8}{\underset{c}{\rightleftharpoons}}$	• $\overset{c}{\underset{159}{\rightleftharpoons}}$	$\overset{c}{\underset{c}{\rightleftharpoons}}$ $\overset{295}{\underset{b}{\rightleftharpoons}}$	•

[a]No mesophase formed.
[b]No transition measured.
[c]No transition detected.

4.5. *Effect of ring size on the thermal behaviour and structural characteristics of the CS mesomorphic state*

To consider how the variation of CS ring size changes thermal phase behaviour and structural properties of their mesophases, we will compare the data discussed in this paper with the results obtained earlier [1] for a series of organocyclotetrasiloxanes *cis*-[PhSi(O)(OSiMe$_2$*R*)]$_4$ with *R* = Me (**I**), CH_2Cl (**Ia**), $CH=CH_2$ (**Ib**). Moreover, we will cite the preliminary results obtained for trimer [PhSi(O)(OSiMe$_3$)]$_3$, which appears to be unable to form a mesophase. Differences between the phase diagrams of CSs with different ring size are presented in table 2, where we combine the data of this paper and the earlier one [1].

An increase of the ring size from tetra- to hexasiloxane, without changes in the side exterior, leads to a broadening of the temperature range of the mesophase. The low temperature boundary of the mesophase shifts to lower temperatures, indicating a reduction in the thermal stability of the crystalline phase; the reason seems to be the higher flexibility of a hexasiloxane ring than that of a cyclotetrasiloxane. One should note the fairly loose molecular packing in the crystalline phase of hexamer **II**; the packing coefficient *k* calculated from the X-ray data for a single crystal [3] is only 0.679. At the same time, the mesophase high temperature limits shifts to higher temperatures. The isotropization of the hexamers cannot be detected as they sublime directly without isotropization above 240–250°C.

Aside from influencing the transition temperatures, the change in CS molecular geometry increases ring flexibility, drastically affecting the mesophase structure. As shown above, the hexamers exhibit polymesomorphic behaviour forming two mesophase modifications in distinct temperature regions within the mesomorphic state. These modifications are structurally different from the tetramer mesophases (table 2).

It is interesting to note the differences in molecular packing for the tetra- and hexamers in the plastically crystalline state. It is known that the densest packing for ellipsoidal molecules is a b.c.c unit cell, while an f.c.c. unit cell is the densest arrangement for globular molecules. As a rule, the molecules of plastic crystals obey this principle [4]. In this respect, the tetramer molecules, having the form of an oblong ellipsoid in the plastically crystalline state, obey this rule too, packing in the b.c.c unit cell. The same situation was observed for the plastically crystalline oligotrimethylsiloxysiloxanes (TMSS) *R*O[Si(O*R*)$_2$O]$_m$*R*, *R*–OSiMe$_3$, with *m* = 2 and 3 [9]. The molecules of hexakistrimethylsiloxydisiloxane (*m* = 2) and octakistrimethylsiloxytrisiloxane (*m* = 3), which possess the form of a prolate ellipsoid,

are arranged in a b.c.c unit cell. In contrast to these examples, the plastically crystalline state of the hexamers is characterized by the formation of an f.c.c. unit cell. This means that the form of hexamer molecules in the HT-mesophase is very close to globular. This fact can be explained only from the point of view discussed earlier in §4.3. The high flexibility of the hexamer ring, as well as the high mobility of side groups, gives a globular form to hexamer molecules at elevated temperatures.

At the same time the trimer appears to be unable to form a plastically crystalline mesophase despite the fact that the shape of its molecules is the closest to spherical, as compared with the tetramers and hexamers. The same behaviour was observed in a TMSS series [9], where the first member ($m=1$)—tetrakistrimethylsiloxisiloxane, $RO[Si(OR)_2O]_mR$, R–$OSiMe_3$, did not show the transition to the plastically crystalline mesophase in spite of its tetrahedron-like molecular form, while the two subsequent members of this series, hexakistrimethylsiloxydisiloxane ($m=2$) and octakistrimethylsiloxytrisiloxane ($m=3$) with ellipsoidal molecules, were plastic crystals in a wide temperature range. (Note that a wealth of known plastic crystals includes an enormous number of compounds with tetrahedron-like molecules [4].)

The mesophase stability for compounds with bulky side groups is most probably supported by a co-operative rotation of molecules. Two factors can be considered responsible for the realization of a co-operative rotation: an ellipsoidal form of a molecule and a great degree of freedom of side groups, the latter to appear without an additional rise of free volume due to the high flexibility of a siloxane ring (in the case of cyclosiloxanes) or a main siloxane chain (in the case of oligotrimethylsiloxysiloxanes). Bulky side groups with a great degree of freedom are able to overlap at the intermolecular level, reducing the undesired free volume.

5. Conclusion

The tetramers **I**, **Ia** and **Ib** and the hexamers **II**, **IIa** and **IIb** have broken several records set up by OPCTS ($MM=745.2$, $\Sigma\Delta V_i=745.2$ Å^3) in 1975 [10] and by two compounds from the TMSS series: hexakistrimethylsiloxydisiloxane and octakistrimethylsiloxytrisiloxane ($MM=607.31$, 829.77 and $\Sigma\Delta V_i=619.1$, 836.7 Å^3, respectively) in 1989 [8] among the plastically crystalline compounds. The cyclosiloxanes **I**, **Ia**, **Ib**, **II**, **IIa** and **IIb** with molecular weights of 841.52, 979.30, 889.56, 1262.28, 1468.95, 1334.34, and $\Sigma\Delta V_i=804.5$, 863.9, 853.9, 1206.8, 1295.9, 1280.9 Å^3, respectively, are by far the largest plastic crystals reported to date. The temperature region of their mesophase existence is substantially larger than in other previously studied plastic crystals. Moreover, the mesomorphic hexamers appear to possess unique properties unusual for plastic crystals with 3D-ordering, viz. the ability to form a second LT-mesomorphic modification with lower (2D) dimensionality of order.

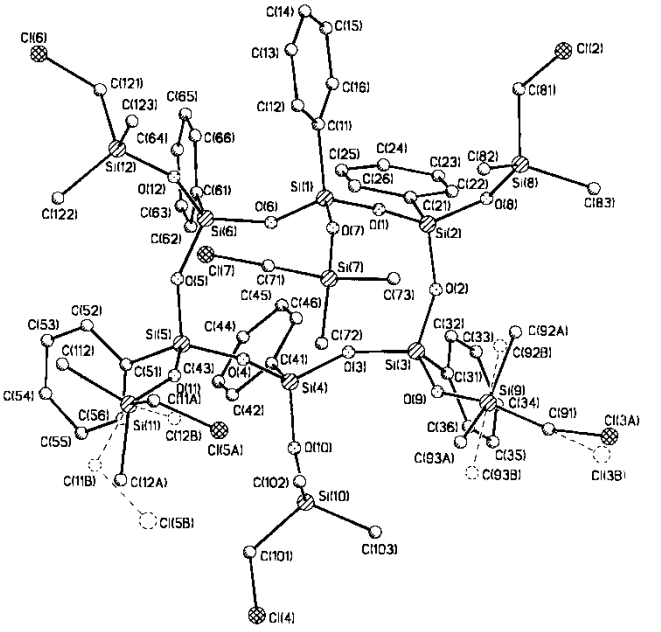

Figure 13. The general view of $[PhSi(O)OSiMe_2(CH_2Cl)]_6$ (**IIa**). The dashed lines show the disordered positions of $SiMe_2CH_2Cl$ groups.

Financial support of this work by Dow Corning Corporation is gratefully acknowledged. The X-ray and DSC investigations were carried out within the project 'INTAS 2000-00525'.

Appendix

The molecular structure of *cis*-$[PhSi(O)OSiMe_2(CH_2Cl)]_6$ (**IIa**) is shown in figure 13 along with selected bond lengths and angles. The conformation of the 12-membered ring is a chair with a deviation of the Si(1) and Si(4) atoms by 1.51 and −0.91 Å from the Si(2)Si(3)Si(5)Si(6) plane. The principal geometry of **IIa** is characterized by values typical for this class of compound [3]. The Si–O exo- and endo-cyclic bonds vary in the narrow range 1.602(2)–1.619(2) Å. The silicon atoms are characterized by a slightly distorted tetrahedral configuration with bond angles from 106.2(1)° to 112.9(2)°. In contrast the Si–O–Si bond angles are characterized by a significant variation, with a maximum value of 173.43(15)° for the Si(2)–O(1)–Si(1) angle, thus indicating a high degree of siloxane ring flexibility.

Analysis of crystal packing has revealed that the molecules are arranged into layers parallel to the

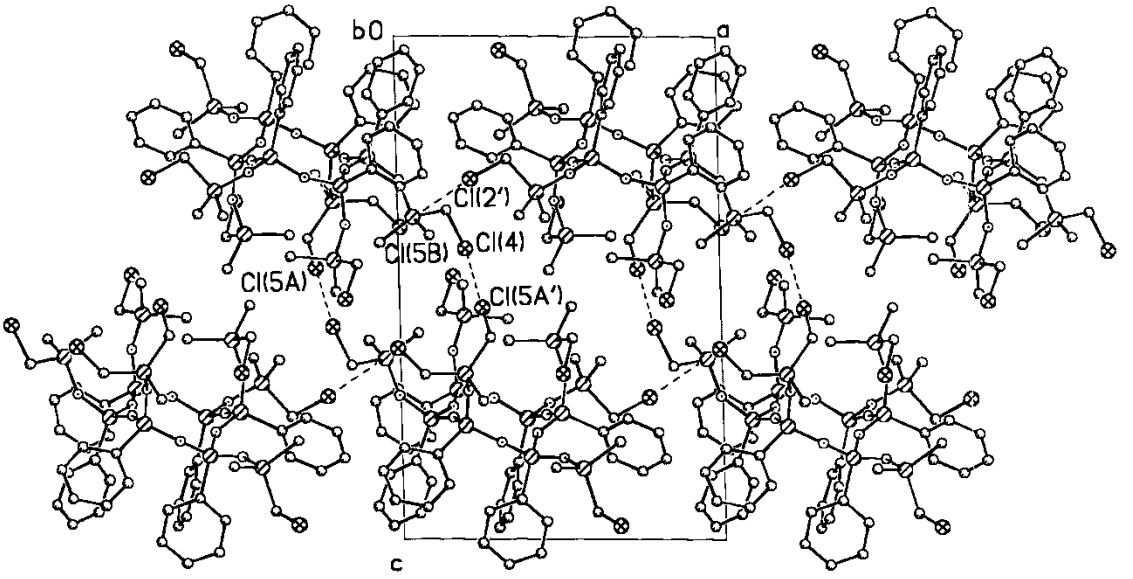

Figure 14. Scheme illustrating the formation of hydrophobic/hydrophilic coated layers and inter- and intra-layers Cl. Cl contacts in **IIa**.

crystallographic *bc* plane (figures 11, 14). In these layers molecules are assembled by the secondary Cl···Cl contacts between the Cl(5A) [one of the orientations of the Si(11)Me_2(CH_2Cl) group] and Cl(4) atoms of adjacent molecules in the layer. In contrast, the Cl(5B) atom corresponding to the other orientation of the disordered Si(11)Me_2(CH_2Cl) group interlinks layers into a double layer structure with the hydrophobic coating (Ph groups) by Cl(5B)···Cl(2) contact. It is noteworthy that these contacts are characterized not only by the shortening of the Cl···Cl distance by up to 3.497(5)–3.516(5) Å but by a specific direction of the contacts, which is reflected in the proximity of the C(11A)Cl(5A)Cl(4) and Cl(5B)Cl(4′)C(93′) angles (179.4(4)° and 170.1(4)°) to 180°. So, it is possible to conclude that Cl···Cl contacts in **IIa** correspond to the transfer of a chlorine electron lone pair to the antibonding C–Cl orbital. The other interactions between these double layers correspond to the normal dispersion interactions of Ph groups.

Crystallographic data for **IIa**: at 110 K, $C_{54}H_{78}Cl_6O_{12}Si_{12}$, $M=1469.2$, Triclinic, space group $P\bar{1}$, $a=13.327(5)$ Å, $b=13.624(5)$ Å, $c=20.867(8)$ Å, $\alpha=78.961(7)°$, $\beta=86.546(8)°$, $\gamma=80.104(7)°$, $V=3662(2)$ Å^3, $Z=2$, $M=1468.94$, $d_{calc}=1.332$ g cm^{-3}, $\mu(MoK_\alpha)=4.83$ cm^{-1}, F(0 0 0) = 1536. The intensities of 29 321 reflections were measured with a Smart 1000 CCD diffractometer at 110 K ($\lambda(MoK_\alpha)=0.71073$ Å, ω-scans with 0.3° step in ω and 10 s per frame exposure, $2\theta<58°$), and 18 231 (R(int) = 0.0239) independent reflections were used in further refinement. The structure was solved by the direct method and refined by the full-matrix least-squares technique against F^2 in the anisotropic–isotropic approximation. The analysis of the Fourier electron density synthesis has revealed that two $SiMe_2CH_2Cl$ groups are disordered by two positions which were included in the refinement in anisotropic approximation. The positions of the hydrogen atoms were calculated geometrically and refined in the riding model. The refinement converged to $wR2=0.0884$ and $GOF=1.083$ for all independent reflections ($R1=0.0619$ was calculated against F for 12 399 observed reflections with $I>2\,\sigma(I)$). The number of the refined parameters was 826. All calculations were performed using SHELXTL PLUS 5.1 on IBM PC AT.

References

[1] Matukhina, E. V., Shchegolikhina, O. I., Pozdniakova, Yu. A., Makarova, N. N., Katsoulis, D. E., and Godovsky, Yu. K., 2001, *Liq. Cryst.*, **28,** 869.

[2] (*a*) Shchegolikhina, O. I., Zhdanov, A. A., Igonin, V. A., Ovchinnikov, Yu. E., Shklover, V. E., and Struchkov, Yu T., 1991, *Metalloorg. Khim.*, **4,** 74, for English translation see (1991) *Organometal. Chem. USSR*, **4,** 39; (*b*) Shchegolikhina, O. I., Pozdnyakova, Yu. A., Molodtsova, Yu. A., Korkin, S. D., Bukalov, S. S., Leites, L. A., Lyssenko, K. A., Peregudov, A. S., Auner, N., and Katsoulis, D. E., 2002, *Inorg. Chem.*, **41,** 6892.

[3] Shchegolikhina, O. I., Igonin, V. A., Molodtsova, Yu. A., Pozdniakova, Yu. A., Zhdanov, A. A., Strelkova, T. V., and Lindeman, S. V., 1998, *J. oganomet. Chem.*, **542,** 141.

[4] Sherwood, N. (editor), 1979, *The Plastically Crystalline State* (New York, London: Wiley).

[5] Post, B., Schwartz, R. S., and Fankuchen, I., 1951, *J. Am. chem. Soc.*, **73,** 5113.

[6] Jackson, R. L., and Strange, J. H., 1972, *Acta Cryst.*, **B28,** 1645.

[7] Kitaigorodsky, A. I., 1973, *Molecular Crystals and*

Molecules, No. 29 in a series 'Physical chemistry' edited by Ernest M. Loebl (New York, London Academic Press).
[8] PERSHIN, V. K., and PERSHIN VL, K., 1979, *Solid State Physics*, **21,** 2292.
[9] MATUKHINA, E. V., KUZMIN, N. N., and ANTIPOV, E. M., 1989, *Dokl. Akad. Nauk. SSSR*, **304,** 904.
[10] KEYES, P. H., and DANIELS, W. B., 1975, *J. chem. Phys.*, **62,** 2000.